Competitive epidemic spreading over arbitrary multilayer networks

Faryad Darabi Sahneh* and Caterina Scoglio
Electrical and Computer Engineering Department, Kansas State University, Manhattan, Kansas 66506, USA
and Institute of Computational Comparative Medicine, Kansas State University, Manhattan, Kansas 66506, USA
(Received 30 August 2013; published 30 June 2014)

This study extends the Susceptible-Infected-Susceptible (SIS) epidemic model for single-virus propagation over an arbitrary graph to an Susceptible-Infected by virus 1-Susceptible-Infected by virus 2-Susceptible (SI_1SI_2S) epidemic model of two exclusive, competitive viruses over a two-layer network with generic structure, where network layers represent the distinct transmission routes of the viruses. We find analytical expressions determining extinction, coexistence, and absolute dominance of the viruses after we introduce the concepts of *survival threshold* and *absolute-dominance threshold*. The main outcome of our analysis is the discovery and proof of a region for long-term coexistence of competitive viruses in nontrivial multilayer networks. We show coexistence is impossible if network layers are identical yet possible if network layers are distinct. Not only do we rigorously prove a region of coexistence, but we can quantitate it via interrelation of central nodes across the network layers. Little to no overlapping of the layers' central nodes is the key determinant of coexistence. For example, we show both analytically and numerically that positive correlation of network layers makes it difficult for a virus to survive, while in a network with negatively correlated layers, survival is easier, but total removal of the other virus is more difficult.

DOI: 10.1103/PhysRevE.89.062817 PACS number(s): 89.75.−k, 89.20.−a, 87.23.Cc

I. INTRODUCTION

Multiple viral spreading within a single population involves very rich dynamics [1], attracting substantial attention [2–4]. Moreover, applications of these types of models extend beyond physiological viruses, as "virus" may refer to products [5], memes [6,7], or pathogens [8,9], for example. However, multiple virus propagation is a mathematically challenging problem. One source of complexity of this problem is multiple interaction possibilities among viruses. For example, viruses may be reinforcing [10], weakening [11], exclusive [12], or asymmetric [3,13].

In the competitive spreading scenario, if infected by one virus, a node (individual) cannot be infected by the other virus. This type of model has implications in such applications as product adoption (e.g., Apple vs Android smart phones), virus-antidote propagation, meme propagation, opposing opinions propagation, and so on. Several researchers have addressed this problem. Newman [12] employed bound percolation to study the spread of two Susceptible-Infected-Removed (SIR) viruses in a host population through a single contact network where a virus takes over the network, then a second virus spreads through the resulting residual network. The paper proved a coexistence threshold above the classical epidemic threshold, indicating the possibility of coexistence in the SIR model. Karrer and Newman [1] extended the work to the more general case where both viruses spread simultaneously. Poletto *et al.* [9] studied the impact of mobility patterns on propagation of two competitive SIR pathogens within a host population. For SIS epidemic spreading, Wang *et al.* [14] studied competitive viruses and proved that exclusive, competitive SIS viruses cannot coexist in scale-free networks. Moreover, for an arbitrary network, Prakash *et al.* [15] proved that competitive SIS virus cannot coexist. Meanwhile, Beutel *et al.* [16] showed coexistence of viruses in the case of SIS viruses with partial immunity (where a node can be infected by both viruses simultaneously).

The competitive spreading problem becomes particularly complicated if the network layers through which viruses propagate are distinct. Current knowledge of how hybridity of underlying topology influences the fate of pathogens is very limited. These systems are usually mathematically intractable, hindering conclusive results on spreading of multiple viruses on multilayer networks. Funk and Jansen [2] extended the bond percolation analysis of two competitive viruses to the case of a two-layer network, investigating effects of layer overlapping. Granell *et al.* [11] studied the interplay between disease and information copropagation in a two-layer network consisting of one physical contact network spreading the disease and a virtual overlay network propagating information to stop the disease. They found a metacritical point for the epidemic onset leading to disease suppression. Importantly, this critical point depends on awareness dynamics and the overlay network structure. Wei *et al.* [17] studied SIS spreading of two competitive viruses on an arbitrary two-layer network, deriving sufficient conditions for exponential die out of both viruses. They also introduced a statistical tool, EigenPredict, to predict viral dominance of one competitive virus over the other [4].

In this paper, we address the problem of two competitive viruses propagating in a host population where each virus has a distinct contact network for propagation. Specifically, we study an SI_1SI_2S model as the simplest extension of the SIS model for single-virus propagation to competitive spreading of two viruses on a two-layer network. From a topology point of view, our study is comprehensive because our multilayer network is allowed to have any arbitrary structure.

Our paper is most relevant to research in [17] and [4]. Wei *et al.* conjectured in [17] and numerically observed in [4] that "*the meme whose first eigenvalue* [18] *is larger tends to prevail eventually in the composite networks.*" However, we challenge this argument in two respects. First, the definition

*faryad@ksu.edu

of viral dominance in [4] is related to comparison of fractions of nodes infected by each virus. However, for two viruses with two different contact networks, having a larger first eigenvalue is not a direct indicator of a higher final fraction of infected nodes. In fact, it is possible to create two distinct network layers where a meme spreading in the population with a smaller first eigenvalue takes over a much larger fraction of the population. Therefore, we find that the definition of viral dominance presented in [4] cannot be corroborated with eigenvalues without restriction to a specific family of networks.

Second, and of paramount interest in this paper, first eigenvalues are graph properties [19] of each layer in isolation, with no information about layers interrelation, and thus cannot capture the joint influence of the network layers, unless some sort of symmetry or homogeneity is assumed. In fact, the generation of one layer in their synthetic multilayer network via the Erdős Réyni model [4] dictated a homogeneity in their multilayer networks, creating a biased platform for further observations of layer interrelations. Our work characterizes the competitive spreading problem more accurately than that presented by Wei *et al.* [4], as our analytical results clearly express the effect of layers' interrelation.

The main outcome of our analysis is discovery and proof of a region for long-term coexistence of competitive viruses in nontrivial multilayer networks. Interestingly, the coexistence region cannot be attributed to any single-layer contact network topology. We show that when the contact graphs of each virus are the same, i.e., the contact network is single-layer, either both viruses die out, or there is only one absolute winner. In other words, it is not possible for both viruses to survive in the long term over a single-layer contact network. Furthermore, the winner is solely determined by epidemic-related parameters, irrespective of the underlying contact topology. However, when the contact graphs are distinct, i.e., the contact topology is a two-layer network, a new phenomenon emerges: Both viruses can coexist long term. Furthermore, the fate of the viruses depends on epidemic-related parameters as well as on the topology of the multilayer network. In particular, we show no or little overlapping of central nodes across the layers is a key determinant of coexistence.

Our results are not limited to any homogeneity assumption or degree distribution or to any network model arguments. Our analytical results determine extinction, coexistence, and absolute dominance of the viruses by introducing concepts of survival threshold and absolute-dominance threshold. Furthermore, for numerical simulations, we employ a multilayer network generation framework to obtain a set of networks so that individual layers have identical graph properties while the interrelation of network layers varies. Therefore, any difference in outputs is purely the result of interrelation. Thus, we offer a paradigmatic contribution to shed light on topology hybridity in multilayer networks.

II. COMPETITIVE SPREADING IN MULTILAYER NETWORKS

In this paper, we study a continuous time SI_1SI_2S model of two competitive viruses propagating on a two-layer network, initially proposed in discrete time [17,20].

A. Multilayer network topology

Consider a population of size N among which two viruses propagate, acquiring distinct transmission routes. For example, an airborne pathogen and a blood-borne pathogen spread within a population through different transmission routes. Represented mathematically, the network topology is a multilayer network because two link types are present; one type allows transmission of virus 1, and the other type allows transmission of virus 2. We represent this multilayer network as $\mathcal{G}(V,E_A,E_B)$, where V is the set of vertices (nodes) and E_A and E_B are sets of edges (links). With labeled vertices from 1 to N, adjacency matrices $A \triangleq [a_{ij}]_{N\times N}$ and $B \triangleq [b_{ij}]_{N\times N}$ correspond to edge sets E_A and E_B, respectively, where $a_{ij}=1$ if node j can transmit virus 1 to node i; otherwise, $a_{ij}=0$, and similarly $b_{ij}=1$ if node j can transmit virus 2 to node i; otherwise, $b_{ij}=0$. We assume the network layers are symmetric, i.e., $a_{ij}=a_{ji}$ and $b_{ij}=b_{ji}$. Corresponding to adjacency matrices A, we define $\boldsymbol{d}_A$ as the node-degree vector, i.e., $d_{A,i}=\sum_{j=1}^{N} a_{ij}$, $D_A \triangleq \mathrm{diag}\{\boldsymbol{d}_A\}$ as the diagonal matrix of node degrees, $\lambda_1(A)$ as the largest eigenvalue (or spectral radius) of A, and $\boldsymbol{v}_A$ as the normalized dominant eigenvector, i.e., $A\boldsymbol{v}_A=\lambda_1(A)\boldsymbol{v}_A$ and $\boldsymbol{v}_A^T\boldsymbol{v}_A=1$. We similarly define $\boldsymbol{d}_B$, D_B, $\lambda_1(B)$, and $\boldsymbol{v}_B$ for adjacency matrix B.

Unlike simple, single-layer graphs, multilayer networks are rather new in network science. To begin, we define simple graphs as $G_A(V,E_A)$ and $G_B(V,E_B)$ to refer to each isolated layer of the multilayer network $\mathcal{G}(V,E_A,E_B)$. This allows us to argue multilayer network $\mathcal{G}$ in terms of simple graph G_A and G_B properties and their *interrelation*. Figure 1 shows a schematic of the two-layer network.

B. SI_1SI_2S model

The SI_1SI_2S model is an extension of continuous-time SIS spreading of a single virus on a simple graph [21,22] to modeling of competitive viruses on a two-layer network. In this model, each node is either "*Susceptible*," "I_1-*Infected*," or "I_2-*Infected*" (i.e., infected by virus 1 or 2, respectively), while virus 1 spreads through E_A edges and virus 2 spreads through E_B edges.

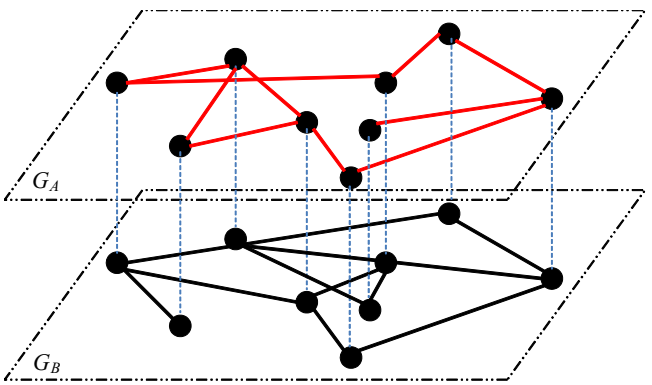

FIG. 1. (Color online) Schematic of two-layer contact topology $\mathcal{G}(V,E_A,E_B)$, where a group of nodes shares two distinct interactions. In our SI_1SI_2S model, virus 1 transmits exclusively via E_A links (red) while virus 2 transmits only through E_B links (black). Dotted vertical lines reiterate that individual nodes are the same in both layers of $\mathcal{G}$.

In this competitive scenario, the two viruses are exclusive: *A node cannot be infected by virus* 1 *and virus* 2 *simultaneously*.

Consistent with SIS propagation on a single graph (cf. [21,22]), the infection and curing processes for viruses 1 and 2 are characterized by (β_1,δ_1) and (β_2,δ_2), respectively. To illustrate, the curing time for I_1-infected node i has an exponential distribution characterized by curing rate $\delta_1 > 0$. The infection of a susceptible node i is a Poisson process which effectively occurs at rate $\beta_1 Y_i(t)$, where $Y_i(t)$ is the number of I_1-infected neighbors of node i at time t in layer G_A. The *effective infection rate* of a virus, defined as the ratio of the infection rate over the curing rate, measures the expected number of attempts of an infected node to infect its neighbor before recovering [23], thus quantifying contagiousness of a virus per contact. Curing and infection processes for virus 2 are similarly described. Figure 2 diagrams the SI_1SI_2S competitive epidemic spreading model over a two-layer network.

The SI_1SI_2S model is essentially a coupled Markov process. For a network with arbitrary structure, this model becomes mathematically intractable due to the exponential explosion of its Markov state space size [24]. To overcome this issue with coupled Markov processes, it is common to apply closure techniques resulting in approximate models with much smaller state space size; however, this is at the expense of accuracy. Specifically, a first order mean-field type approximation [24] suggests the following differential equations for the evolution of infection probabilities of viruses 1 and 2, denoted by $p_{1,i}$ and $p_{2,i}$ for node i, respectively,

$$\dot{p}_{1,i} = \beta_1(1 - p_{1,i} - p_{2,i}) \sum_{j=1}^{N} a_{ij} p_{1,j} - \delta_1 p_{1,i}, \quad (1)$$

$$\dot{p}_{2,i} = \beta_2(1 - p_{1,i} - p_{2,i}) \sum_{j=1}^{N} b_{ij} p_{2,j} - \delta_2 p_{2,i}, \quad (2)$$

for $i \in \{1,\ldots,N\}$, with the state-space size of $2N$. This model is an extension of the NIMFA model [21] for SIS spreading on simple graphs.

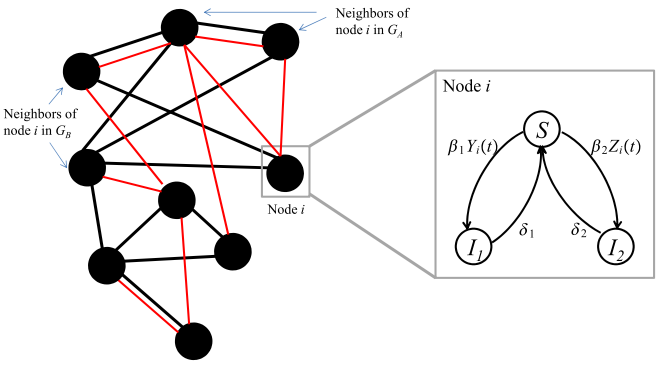

FIG. 2. (Color online) Schematic of a contact network with the node-level stochastic transition diagram for node i, according to the SI_1SI_2S epidemic spreading model. Parameters β_1 and δ_1 denote virus 1 infection rate and curing rate, respectively, and $Y_i(t)$ is the number of node i neighbors in layer G_A infected by virus 1 at time t. Similarly, β_2 and δ_2 denote virus 2 infection rate and curing rate, respectively, and $Z_i(t)$ is the number of node i neighbors in layer G_B infected by virus 2 at time t.

Our competitive virus propagation model [Eqs. (1) and (2)] exhibits rich dynamical behavior dependent on epidemic parameters and contact network multilayer structure. Accordingly, values of effective infection rates $\tau_1 \triangleq \frac{\beta_1}{\delta_1}$ and $\tau_2 \triangleq \frac{\beta_2}{\delta_2}$ of viruses 1 and 2 yield several possible outcomes for the SI_1SI_2S model [Eqs. (1) and (2)]. In particular, both viruses may become extinct ultimately, or one can remove the other one, or both will coexist.

C. Problem statement

Linearization of our SI_1SI_2S model [Eqs. (1) and (2)] at the healthy equilibrium (i.e., $p^*_{1,i} = p^*_{2,i} = 0, i \in \{1,\ldots,N\}$) demonstrates the exponential extinction condition for both viruses. When $\tau_1 < 1/\lambda_1(A)$ and $\tau_2 < 1/\lambda_1(B)$, any initial infections exponentially die out. In this paper, we refer to such critical value as a *no-spreading threshold* because a virus with a lower effective infection rate is too weak to spread in the population even in the absence of any viral competition.

Wei *et al.* [17] detailed the no-spreading condition: If $\tau_1 < 1/\lambda_1(A)$, virus 1 does not spread and exponentially dies out. Importantly, exponential extinction of both viruses occurs only if $\tau_1 < 1/\lambda_1(A)$ and $\tau_2 < 1/\lambda_1(B)$ simultaneously. Also, dynamical interplay between the competitive viruses does not affect the no-spreading thresholds $\tau_1^0 = 1/\lambda_1(A)$ and $\tau_2^0 = 1/\lambda_1(B)$ for virus 1 and virus 2. These thresholds remain independent of virus competition characteristics and network layer interrelation. Exponential extinction is the only analytical outcome in Wei *et al.* [17]. If the effective infection rate of one of the viruses is below its no-spreading threshold, the competitive spreading problem reduces to single-virus propagation. However, our paper addresses the case where for both viruses $\tau_1 > 1/\lambda_1(A)$ and $\tau_2 > 1/\lambda_1(B)$. In this case, the healthy equilibrium is unstable, and consequently at least one of the two viruses persists.

Problem I. Assume the effective infection rates of each virus are larger than their no-spreading threshold, i.e., $\tau_1 > 1/\lambda_1(A)$ and $\tau_2 > 1/\lambda_1(B)$.

(1) Will both viruses survive (coexistence), or will one virus completely remove the other (absolute dominance)?

(2) Which characteristics of a multilayer network structure allow for coexistence?

This problem is essentially a two-virus problem, and so we are interested in predicting what happens to the viruses for given values of the pair (τ_1,τ_2). Will both die out? Will one dominate the other? Will both coexist? To answer these questions, we focus only on one virus instead of studying the two viruses at the same time. With no loss of generality, we choose virus 1. In this approach, we consider virus 2 as an external factor reducing the susceptibility of the population for virus 1. Therefore, instead of the initial two-virus problem, we study the fate of virus 1 given that virus 2 has the capability to infect the population and its effective infection rate is $\tau_2 > 1/\lambda_1(B)$. We investigate whether virus 1 dies out or it survives when competing with virus 2. In case it survives, it may coexist with virus 2, or it may be the absolute winner, removing virus 2 completely from the population. Formally, solving the two-virus problem boils down to studying the fate of virus 1 given virus 2.

Problem II. Assume that the effective infection rate of virus 2 is τ_2 and that it is greater than the no-spreading threshold of virus 2, i.e., $\tau_2 > 1/\lambda_1(B)$.

(1) For which values of τ_1 will virus 1 survive?

(2) For which values of τ_1 will virus 1 survive and be the absolute winner, removing virus 2 completely?

Problem I and Problem II are equivalent. We address Problem II by introducing two critical values for the effective infection rate, namely, *survival threshold* τ_{c1} and *absolute-dominance threshold* $\tau_1^\dagger$. We then argue that absolute-dominance threshold of one virus corresponds to the survival threshold of the other virus. This further simplifies the problem to finding the survival threshold of virus 1.

These questions pertain to long-term behaviors of competitive spreading dynamics. To address these questions, we perform a steady-state analysis of SI_1SI_2S model. Specifically, bifurcation techniques are used to find two critical values, survival threshold and absolute-dominance threshold, determining if a virus will survive and whether it can completely remove the other virus. Significantly, we go beyond these threshold conditions and examine interrelation of network layers. Using eigenvalue perturbation, we find interrelations of dominant eigenvectors and node-degree vectors of network layers are critical determinants in ultimate behaviors of competitive viral dynamics.

III. MAIN RESULTS

Dynamics of the competitive spreading SI_1SI_2S model is rather complicated, and its mathematical analysis might look cumbersome. Therefore, we have moved all the deductions and proofs to the Appendix section and only report the final results. The mathematical tools that we use in this study are equilibrium analysis, bifurcation theory, and the eigenvalue perturbation.

A. Equilibrium analysis and threshold equations

The SI_1SI_2S competitive virus propagation model [Eqs. (1) and (2)] yields the equilibrium equations

$$\frac{p^*_{1,i}}{1-p^*_{1,i}-p^*_{2,i}} = \tau_1 \sum a_{ij} p^*_{1,j}, \tag{3}$$

$$\frac{p^*_{2,i}}{1-p^*_{1,i}-p^*_{2,i}} = \tau_2 \sum b_{ij} p^*_{2,j}, \tag{4}$$

for $i \in \{1,\dots,N\}$, where $p^*_{1,i}$ and $p^*_{2,i}$ are, respectively, virus 1 and virus 2 equilibrium infection probabilities of node i. When $\tau_1 > 1/\lambda_1(A)$ and $\tau_2 > 1/\lambda_1(B)$, equilibrium equations (3) and (4) suggest that the SI_1SI_2S competitive spreading model have *at least* the following three equilibrium points:

(1) disease-free equilibrium $(p^*_{1,i}=0, p^*_{2,i}=0)\ \forall\, i \in \{1,\dots,N\}$, where all the nodes are healthy,

(2) virus 2 absolute-dominance equilibrium $(p^*_{1,i}=0, p^*_{2,i}=y_i>0)\ \forall\, i \in \{1,\dots,N\}$, where nodes are only infected by virus 2,

(3) virus 1 absolute-dominance equilibrium $(p^*_{1,i}=z_i>0, p^*_{2,i}=0)\ \forall\, i \in \{1,\dots,N\}$ where nodes are only infected by virus 1,

where z_i and y_i are steady-state infection probabilities in the case of single-virus propagation (see [21]), satisfying

$$\frac{z_i}{1-z_i} = \tau_1 \sum a_{ij} z_j, \tag{5}$$

$$\frac{y_i}{1-y_i} = \tau_2 \sum b_{ij} y_j, \tag{6}$$

for $i \in \{1,\dots,N\}$.

The disease-free equilibrium $(p^*_{1,i}=0, p^*_{2,i}=0)$ is always unstable for $\tau_1 > 1/\lambda_1(A)$ and $\tau_2 > 1/\lambda_1(B)$. Each of the above three solutions to the equilibrium equation [Eqs. (3) and (4)] corresponds to the case that at least one of the viruses does not exist. Next, to have coexistence of the two viruses, equilibriums (2) and (3) should also be unstable, and a fourth stable equilibrium should exist where $(p^*_{1,i}>0, p^*_{2,i}>0)\ \forall\, i \in \{1,\dots,N\}$. We refer to this equilibrium as *coexistence equilibrium* and show that it only exists for multilayer contact networks.

As explained in Sec. II C, we study this two-virus problem by analyzing virus 1 behavior, considering virus 2 as an external factor. Definitions of survival and absolute-dominance thresholds facilitate our analysis.

Definition. Given virus 2 effective infection rate $\tau_2 > 1/\lambda_1(B)$, the *survival threshold* τ_{1c} is the critical point such that virus 1 steady-state infection probability of each node is zero for $\tau_1 < \tau_{1c}$ and is positive for $\tau_1 > \tau_{1c}$; i.e.,

$$p^{ss}_{1,i} = 0, \quad \text{for } \tau_1 < \tau_{1c},$$
$$p^{ss}_{1,i} > 0, \quad \text{for } \tau_1 > \tau_{1c}.$$

Definition. Given virus 2 effective infection rate $\tau_2 > 1/\lambda_1(B)$, the *absolute-dominance threshold* $\tau_1^\dagger$ is the critical point such that not only virus 1 survives but also it removes the other virus. In other words, virus 2 steady-state infection probability of each node becomes zero for $\tau_1 > \tau_1^\dagger$; i.e.,

$$p^{ss}_{2,i} > 0 \quad \text{for } \tau_1 < \tau_1^\dagger,$$
$$p^{ss}_{2,i} = 0, \quad \text{for } \tau_1 > \tau_1^\dagger,$$

for $\forall\, i \in \{1,\dots,N\}$.

For $\tau_2 \leqslant 1/\lambda_1(B)$, the survival and absolute-dominance conditions coincide and $\tau_{1c} = \tau_1^\dagger = \tau_1^0 = 1/\lambda_1(A)$. It is important to clearly distinguish the difference between the no-spreading threshold and the survival threshold. The no-spreading threshold is the critical value of effective infection rate at which a virus cannot spread in the population, regardless of any competition with another virus. The no-spreading threshold corresponds with the transient dynamics of the spreading. The survival threshold, on the other hand, corresponds with the long-term behavior of a virus, whether it is going to eventually die out or persist in the population. The survival threshold τ_{c1} is larger than the no-spreading threshold because competition with another virus reduces the susceptibility of the population, hence making it more difficult for the virus to survive. Thus, a virus that may initially spread in the population can die out eventually as the other virus grows. For virus 1, this scenario occurs if $\tau_1 > \tau_1^0 = 1/\lambda_1(A)$ and $\tau_1 < \tau_{1c}$.

1. *Case of single-layer network*

If the two layers are identical, i.e., $B = A$, the survival threshold and the absolute-dominance threshold coincide, indicating that a surviving virus is also the absolute winner. Stability analysis of the equilibriums in case of identical network layers (see Sec. 1 of the Appendix) proves that virus 2 absolute-dominance equilibrium ($p^*_{1,i} = 0, p^*_{2,i} = y_i > 0$) is stable if and only if $\tau_1 < \tau_2$. Furthermore, virus 1 absolute-dominance equilibrium ($p^*_{1,i} = z_i > 0, p^*_{2,i} = 0$) is stable if and only if $\tau_2 < \tau_1$. Therefore, for $\tau_1 \neq \tau_2$ exactly one of the absolute-dominance equilibrium points is stable and the virus with larger effective infection rate is the sole survivor. In support, according to the definitions of survival and absolute-dominance thresholds, $\tau_{1c} = \tau_1^\dagger = \tau_2$, denoting an abrupt transition for competitive spreading over a single-layer network. This is consistent with the previous result of [15]. Figure 3 shows the sharp transition for the steady-state infection fractions in the SI_1SI_2S model as a function of τ_1, holding τ_2 fixed at a given value.

2. *Case of multilayer network*

In contrast with the case of single-layer networks, survival threshold and absolute-dominance threshold do not necessarily overlap for multilayer contact network. As a result, there is a nontrivial region for (τ_1, τ_2) values where both viruses exist, which we refer to as the *coexistence region*. Figure 4 shows that the absolute-dominance and survival thresholds are distinct for a two-layer network (see Sec. III E for details of network generation).

Given τ_2, plotting virus 1 steady-state infection fraction $\bar{p}_1^{ss} = \frac{1}{N}\sum_{j=1}^{N} p_{1,i}^{ss}$ as a function of τ_1 identifies the survival threshold τ_{1c} at which $\bar{p}_1^{ss}$ becomes positive. Interestingly, another alternative to identifying the absolute-dominance threshold is to also plot the infection fraction of virus 1 in the absence of any competition with virus 2 ($\tau_2 = 0$). The two curves must coincide for τ_1 larger than the absolute-dominance threshold because for $\tau_1 > \tau_1^\dagger$, virus 2 infection probabilities are zero. Next, Figure 5 illustrates for extinction, coexistence, and absolute-dominance regions for virus 1.

Bifurcation analysis of the SI_1SI_2S equilibriums can determine the survival thresholds. The coexistence scenario corresponds to a coexistence equilibrium for SI_1SI_2S model [Eqs. (1) and (2)], where $(p^*_{1,i} > 0, p^*_{2,i} > 0)\ \forall\ i \in \{1, \ldots, N\}$. Given τ_2, virus 1 survival threshold is the critical value where such coexistence equilibrium emerges. Exactly at the threshold value τ_{1c}, $p^*_{1,i}|_{\tau_1=\tau_{1c}} = 0$ and $\frac{dp^*_{1,i}}{d\tau_1}|_{\tau_1=\tau_{1c}} > 0$ for all $i \in \{1, \ldots, N\}$. Taking the derivative of equilibrium equation (3) with respect to τ_1, and defining

$$w_i \triangleq \left.\frac{dp^*_{1,i}}{d\tau_1}\right|_{\tau_1=\tau_{1c}}, \quad y_i \triangleq p^*_{2,i}|_{\tau_1=\tau_{1c}}, \tag{7}$$

we find that the survival threshold τ_{1c} is the value for which a nontrivial solution exists for $w_i > 0$ in

$$w_i = \tau_{1c}(1 - y_i)\sum a_{ij} w_j, \tag{8}$$

where y_i is the solution of (6). Notably, Eq. (8) is an eigenvalue problem (see Sec. 2 of the Appendix). Among all the possible solutions, only

$$\tau_{1c} = \frac{1}{\lambda_1(\mathrm{diag}\{1-y_i\}A)} \tag{9}$$

is acceptable; according to the Perron-Frobenius theorem, only the dominant eigenvector of the matrix $\mathrm{diag}\{1 - y_i\}A$ has all positive entries, allowing $w_i = \frac{dp^*_{1,i}}{d\tau_1}|_{\tau_1=\tau_{1c}} > 0$. Having $w_i > 0$ at critical point τ_{1c} denotes the emergence of the coexistence equilibrium.

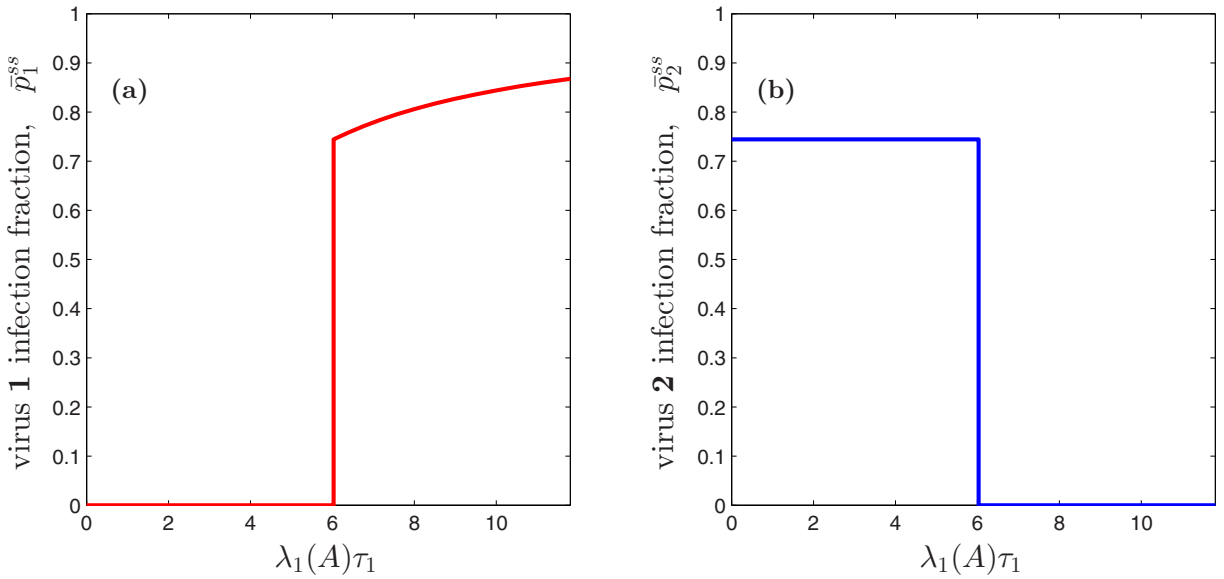

FIG. 3. (Color online) Phase transition of competitive spreading model SI_1SI_2S for a *single-layer* network, i.e., $B = A$. Holding the effective infection rate of virus 2 constant at $\tau_2 = 6\frac{1}{\lambda_1(B)} = 6\frac{1}{\lambda_1(A)}$ and varying τ_1, (a) the steady-state infection fraction of virus 1, $\bar{p}_1^{ss} = \frac{1}{N}\sum p_{1,i}^{ss}$, and (b) the steady-state infection fraction of virus 2, $\bar{p}_2^{ss} = \frac{1}{N}\sum p_{2,i}^{ss}$, exhibit abrupt phase transition at $\tau_1 = 6\frac{1}{\lambda_1(A)} = \tau_2$. Specifically, (a) $\bar{p}_1^{ss}$ is zero for $\tau_1 < \tau_2$ and is positive for $\tau_1 > \tau_2$, denoting survival threshold of virus 1, and (b) $\bar{p}_2^{ss}$ is positive for $\tau_1 < \tau_2$ and becomes zero for $\tau_1 > \tau_2$, indicating absolute removal of virus 2 and thus the virus 1 absolute-dominance threshold.

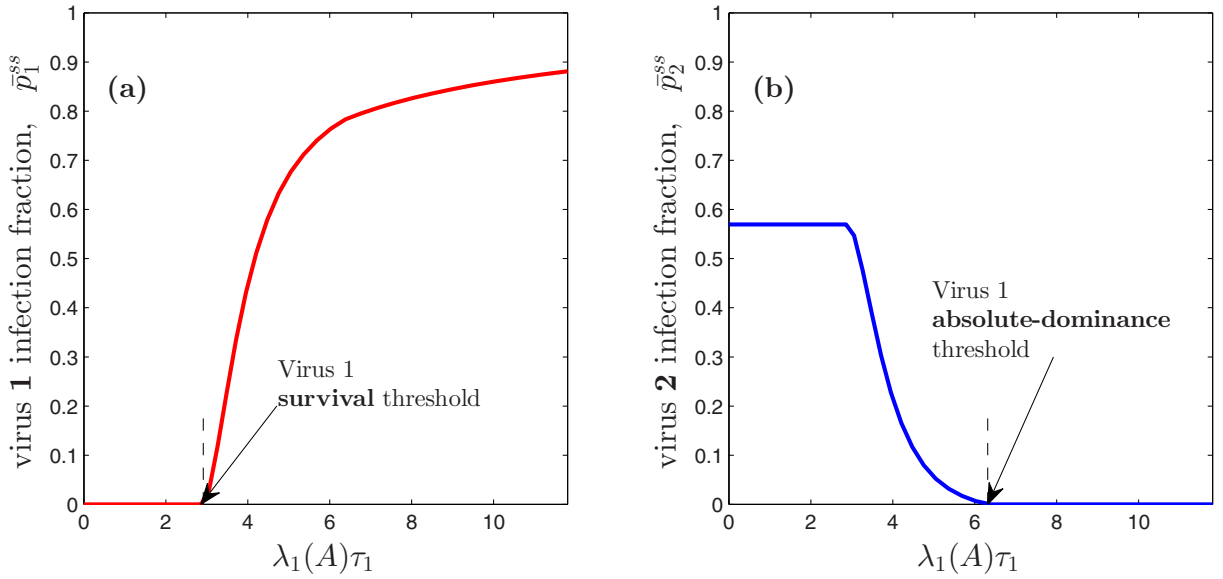

FIG. 4. (Color online) Illustration of survival and absolute-dominance thresholds for virus 1 on a multilayer contact network. Holding the effective infection rate of virus 2 constant at $\tau_2 = 6\frac{1}{\lambda_1(B)}$, (a) the steady-state infection fraction of virus 1, $\bar{p}_1^{ss} = \frac{1}{N}\sum p_{1,i}^{ss}$, and (b) the steady-state infection fraction of virus 2, $\bar{p}_2^{ss} = \frac{1}{N}\sum p_{2,i}^{ss}$, exhibit phase transition at survival threshold τ_{c1} and absolute-dominance threshold $\tau_1^\dagger$, respectively. Specifically, (a) $\bar{p}_1^{ss}$ is zero for $\tau_1 < \tau_{c1}$ and becomes positive for $\tau_1 > \tau_{c1}$, denoting survival threshold of virus 1, and (b) $\bar{p}_2^{ss}$ is positive for $\tau_1 < \tau_1^\dagger$ and becomes zero for $\tau_1 > \tau_1^\dagger$, indicating absolute removal of virus 2 and thus the virus 1 absolute-dominance threshold. Additionally, it is interesting to observe that $\bar{p}_2^{ss}$ is constant when $\tau_1 < \tau_{c1}$ while it reduces gradually as τ_1 becomes larger than τ_{c1}.

As discussed earlier, the survival threshold for virus 1 must be larger than the no-spreading threshold $1/\lambda_1(A)$ as a result of reduced susceptibility due to competition with virus 2. Accordingly, the above formulas for virus 1 survival threshold offer intuitive interpretations. For instance, the expression in (9) demonstrates that susceptibility is reduced by factor $(1 - y_i)$, where according to (6), y_i is the steady-state infection probability of virus 2 in the absence of virus 1 ($\tau_1 = 0$). Similar to the SIS epidemic threshold [21], the survival threshold (9) is the inverse of the spectral radius of the adjacency matrix A but scaled by the reduced susceptibility factor $(1 - y_i)$ for each node.

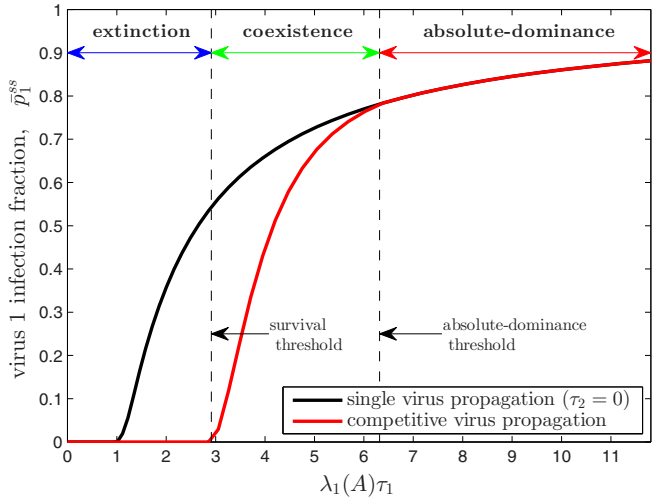

FIG. 5. (Color online) Steady-state infection fraction curve of virus 1 in the SI_1SI_2S competing spreading model (red). While increasing τ_1, the steady-state infection fraction of virus 1 in the SI_1SI_2S model becomes nonzero at the survival threshold τ_{1c}, while it coincides with that of the SIS model (black curve) at the absolute-dominance threshold $\tau_1^\dagger$. In this simulation, the steady-state infection fraction of virus 1 ($\bar{p}_1^{ss}$) is zero for $\tau_1 \leqslant \tau_{1c} \simeq 3\frac{1}{\lambda_1(A)}$, an extinction region for virus 1. Interestingly, for $\tau_1 > \tau_1^\dagger \simeq 6.6\frac{1}{\lambda_1(A)}$, $\bar{p}_1^{ss}$ for the competitive scenario (red curve) is identical to the case of single-virus propagation (black curve), suggesting extinction of virus 2, hence marking this region the absolute-dominance range for virus 1. For $\tau_1 \in (\tau_{1c}, \tau_1^\dagger)$, virus 1 and virus 2 both persist in the population, marking this range a coexistence region.

By the duality of expressions, the virus 2 survival threshold is $\tau_{2c} = 1/\lambda_1(\mathrm{diag}\{1 - z_i\}B)$, where z_i is the solution of (5) denoting virus 1 infection fraction in the absence of any competition with virus 2 ($\tau_2 = 0$). The bifurcation analysis thus shows that if $\tau_1 > \tau_{1c}$ and $\tau_2 > \tau_{2c}$, then the SI_1SI_2S model [Eqs. (1) and (2)] has a coexistence equilibrium $(p_{1,i}^* > 0, p_{2,i}^* > 0)\ \forall\ i \in \{1, \ldots, N\}$. In this case, all the other equilibriums of the system are unstable (see Sec. 2 of the Appendix).

The bifurcation analysis for finding the survival threshold for a two-layer network does not apply to the case of single-layer network, where the transition is abrupt. However, we can show that $\tau_{1c} = \tau_2$ and $w_i = cy_i$ solve the Perron-Frobenius problem (8). However, further analysis shows $c = 0$, implying that coexistence equilibrium does not emerge in case of single-layer networks.

Next, the survival and absolute-dominance thresholds of virus 1 are functions of τ_2, which we denote by $\tau_{1c} = \Phi_1(\tau_2)$ and $\tau_1^\dagger = \Psi_1(\tau_2)$. Similarly, for virus 2, we can define survival and absolute-dominance thresholds $\tau_{2c} = \Phi_2(\tau_1)$ and $\tau_2^\dagger = \Psi_2(\tau_1)$. Here the absolute-dominance threshold of one virus is closely related to the survival threshold of the other virus.

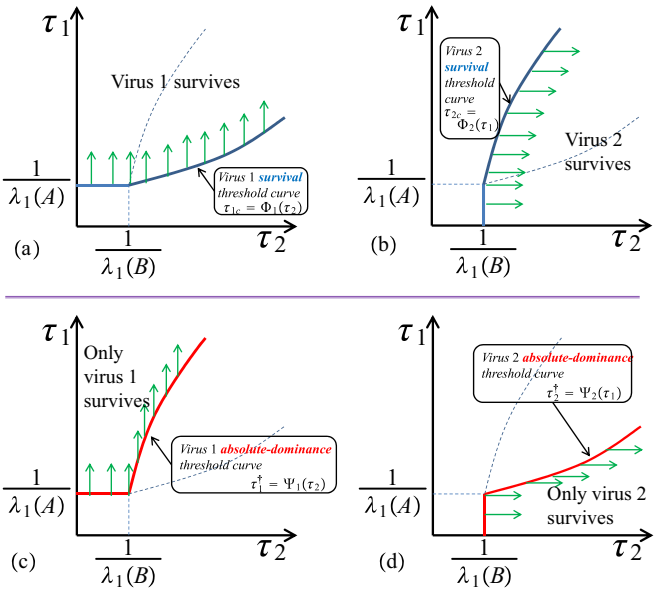

FIG. 6. (Color online) Illustration of survival and absolute-dominance threshold curves in the SI_1SI_2S model. (a) Virus 1 survives if its effective infection rates is larger than the survival threshold, i.e., $\tau_1 > \tau_{c1} = \Phi_1(\tau_2)$. A similar argument holds for the survival threshold curve of virus 2, as depicted in (b). The absolute-dominance threshold curves can be obtained from the survival curves shown in (a) and (b). Specifically, the region virus 1 is the absolute winner is where virus 1 survives and virus 2 does not survive, as shown in (c). Likewise, the region virus 2 is the absolute winner is where virus 1 does not survive while virus 2 survives (d).

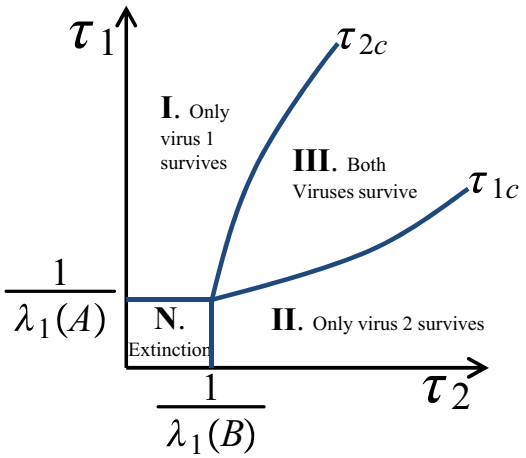

FIG. 7. (Color online) The SI_1SI_2S model with two-layer contact topology exhibits four possibilities: extinction region N, where both viruses die out; virus 1 absolute-dominance region I, where virus 1 survives and virus 2 dies out; virus 2 absolute-dominance region II, where virus 2 survives and virus 1 dies out; and, finally, coexistence region III, where both viruses survive and persist in the population.

Specifically, virus 1 absolute-dominance condition $\tau_1 > \tau_1^\dagger$ is equivalent to virus 2 extinction condition $\tau_2 < \tau_{2c}$. Therefore, for $\tau_1 > 1/\lambda_1(A)$ and $\tau_2 > 1/\lambda_1(B)$,

$$\Psi_1(\tau_2) = \Phi_2^{-1}(\tau_2). \tag{10}$$

Figure 6 illustrates the survival and absolute-dominance threshold curves of the two viruses, clarifying the above relationship graphically.

The threshold curves identify four regions in the (τ_1, τ_2) plane where both viruses die out, virus 1 survives only, virus 2 survives only, or both survive and coexist. Figure 7 depicts a typical phase diagram of SI_1SI_2S competitive spreading on two-layer contact networks.

The eigenvalue problem (8) gives a mathematical way to find the survival threshold τ_{1c}, depending on the value of τ_2. Unfortunately, this implicit dependence hinders clear understanding of the propagation interplay between virus 1 and virus 2. Particularly, the role of the multilayer contact topology and layer interrelations on the competitive spreading is not apparent. In the following section, we employ eigenvalue perturbation techniques to unravel the multilayer network role.

B. Characterization of threshold curves

Since complete analytical solution of survival threshold curves is not feasible, instead, we can characterize the threshold curves through explicit analytical quantities. Our approach to this problem finds explicit solutions to (9) for values of τ_2 close to $1/\lambda_1(B)$ and for very large values of τ_2 to quantitate the survival epidemic curves. Since we know the solution to (6) and the survival threshold value τ_{1c} at both extreme values, we can employ eigenvalue perturbation techniques to find explicit solutions for τ_2 close to $1/\lambda_1(B)$ and τ_2 very large. Results for τ_2 close to $1/\lambda_1(B)$ apply where competitive viruses are *nonaggressive*, whereas results for very large τ_2 corresponds to *aggressive* [25] competition. Even though there is no clear phase transition between aggressive and nonaggressive competition, these extreme scenarios qualitatively describe the competition behavior when effective infection rates of the viruses are much larger than their respective no-spreading threshold, as well as when they are just moderately above the no-spreading thresholds. Behavior of competitive spreading processes is an interpolation of the extreme scenarios of nonaggressive and aggressive propagation.

First, we perform perturbation analysis to find τ_{c1} for values of τ_2 close to $1/\lambda_1(B)$. We know thatt at $\tau_2 = 1/\lambda_1(B)$, $y_i = 0$ solves (6); thus, $\tau_{c1} = 1/\lambda_1(A)$ is the survival threshold according to (9). For values of τ_2 close to $1/\lambda_1(B)$, we use eigenvalue perturbation technique and study the sensitivity of threshold equation (8) respective to deviation in τ_2 from $1/\lambda_1(B)$. As detailed in Sec. 3 of the Appendix, we find

$$\left.\frac{d\tau_{1c}}{d\tau_2}\right|_{\tau_2=\frac{1}{\lambda_1(B)}} = \frac{\lambda_1(B)}{\lambda_1(A)} \frac{\sum v_{A,i}^2 v_{B,i}}{\sum v_{B,i}^3}, \tag{11}$$

expressing the dependency of virus 1 survival threshold (τ_{1c}) to effective infection rate of virus 2 (τ_2) for values of τ_2 close to $1/\lambda_1(B)$. In the above equation, $v_{A,i}$ and $v_{B,i}$ are the ith element of normalized dominant eigenvectors $\boldsymbol{v}_A$ and $\boldsymbol{v}_B$ of A and B, respectively. Among the terms in expression (11), $\lambda_1(B)$, $\lambda_1(A)$, and $\sum v_{B,i}^3$ are all graph properties of network layers in isolation, while $\sum v_{A,i}^2 v_{B,i}$ determines the influence of interrelations of the two network layers. Significantly, if $\sum v_{A,i}^2 v_{B,i}$ is small, expression (11) suggests the virus 1 survival threshold is minimally influenced by virus 2 infection

rate. This offers very interesting interpretations: When spectral central nodes of G_A (those nodes with a larger element in dominant eigenvector of G_A) are spectrally insignificant in G_B, the virus 1 survival threshold does not increase much by τ_2. In other words, virus 2 does not compete over accessible resources of virus 1; therefore, virus 1 is not affected much by the copropagation. On the other hand, if spectral central nodes of G_A also have high spectral centrality in G_B, then $\sum v_{A,i}^2 v_{B,i}$ is maximal, indicating considerable dependency of virus 1 survival threshold on the contagiousness of the other virus. From (11), the die-out threshold curve $\Phi_1(\tau_2)$ can be approximated close to $(\tau_2,\tau_1) = [\frac{1}{\lambda_1(B)}, \frac{1}{\lambda_1(A)}]$ as

$$\Phi_1(\tau_2) \simeq \frac{1}{\lambda_1(A)} \left\{ 1 + \frac{\sum v_{A,i}^2 v_{B,i}}{\sum v_{B,i}^3} [\lambda_1(B)\tau_2 - 1] \right\}. \quad (12)$$

Studying threshold equations (8) for $\tau_2 \to \infty$, we find that $\frac{\tau_{1c}}{\tau_2}|_{\tau_2\to\infty}$ is the inverse of the spectral radius of $D_B^{-1}A$ (see Sec. 3 of the Appendix for detailed derivation),

$$\frac{\tau_{1c}}{\tau_2}|_{\tau_2\to\infty} = \frac{1}{\lambda_1\left(D_B^{-1}A\right)} = \frac{1}{\lambda_1\left(D_B^{-1/2}AD_B^{-1/2}\right)}, \quad (13)$$

expressing the dependency of the virus 1 survival threshold (τ_{1c}) on the effective infection rate of virus 2 (τ_2) for large values of τ_2. Expression (13) directly highlights the influence of interrelations of the two layers. Significantly, if $\lambda_1(D_B^{-1}A)$ is large, expression (13) suggests that virus 1 survival threshold does not increase significantly by virus 2 infection rate. Similar arguments about interpretation of nonaggressive competition apply to aggressive competitive viruses where τ_1 and τ_2 are relatively large. The main difference in case of aggressive competitive spreading is that node degree is the determinant of centrality. From (13), the die-out threshold curve $\Phi_1(\tau_2)$ asymptotically becomes

$$\Phi_1(\tau_2) \simeq \frac{1}{\lambda_1\left(D_B^{-1}A\right)}\tau_2 \quad (14)$$

for aggressive competitive propagation. Figure 8 depicts survival threshold curves for nonaggressive (left) and aggressive (right) competitive spreading.

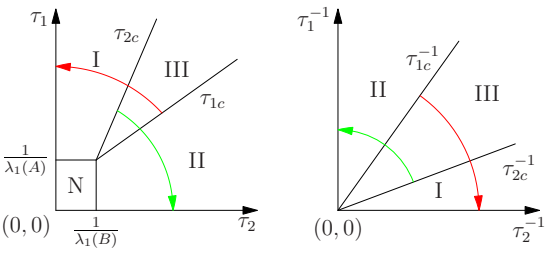

FIG. 8. (Color online) The survival regions diagram in SI_1SI_2S model for values of (τ_1,τ_2) close to $[\frac{1}{\lambda_1(A)}, \frac{1}{\lambda_1(B)}]$ (left) and for very large values of (τ_1,τ_2) (right). Regions N, I, II, and III are as defined in Fig. 7. The red arrow shows the survival region of virus 1 (regions I and III) and the green arrow shows the survival region of virus 2 (regions II and III). For the aggressive viruses scenario, axes have inverse values of (τ_1,τ_2) so that the origin represents infinitely large values. Equations (11) and (13) analytically find the separating lines between the survival regions in explicit expressions.

We prove conditions for coexistence by showing that there is overlapping between regions where viruses survive.

Theorem 1. In the SI_1SI_2S model [Eqs. (1) and (2)] for competitive epidemics over multilayer networks, if the two network layers G_A and G_B are identical, coexistence is impossible; i.e., a virus with even a slightly larger effective infection rate dominates and completely removes the other virus. Otherwise, if node-degree vectors of G_A and G_B are not parallel, i.e., $\boldsymbol{d}_A \nparallel \boldsymbol{d}_B$, or if normalized dominant eigenvectors of G_A and G_B do not completely overlap, i.e., $\boldsymbol{v}_A \neq \boldsymbol{v}_B$, the multilayer structure of the underlying topology allows a nontrivial coexistence region.

Proof. If network layers are identical (i.e., $G_A = G_B$), we show in Sec. III A 1 that survival and absolute-dominance thresholds coincide. Therefore, the virus with even a slightly larger effective infection rate dominates and completely removes the other virus if the two network layers are identical.

To show the possibility of coexistence for nonaggressive competitive viruses, we show that the survival regions overlap by proving

$$\frac{d\tau_{1,c}}{d\tau_2}\frac{d\tau_{2,c}}{d\tau_1}\bigg|_{(\tau_1,\tau_2)=[\frac{1}{\lambda_1(A)},\frac{1}{\lambda_1(B)}]} < 1. \quad (15)$$

Using expression (11) and its counterpart for $\frac{d\tau_{2,c}}{d\tau_1}$, we need to show

$$\frac{\left(\sum v_{B,i}v_{A,i}^2\right)\left(\sum v_{A,i}v_{B,i}^2\right)}{\left(\sum v_{B,i}^3\right)\left(\sum v_{A,i}^3\right)} < 1. \quad (16)$$

As proved in Sec. 4 of the Appendix, we find that condition (15) is always true except for the special case where dominant eigenvectors of G_A and G_B completely overlap, i.e., $\boldsymbol{v}_A = \boldsymbol{v}_B$.

To show the possibility of coexistence for aggressive competitive viruses, we show the survival regions overlap by proving

$$\left(\frac{\tau_{1c}}{\tau_2}\bigg|_{\tau_2\to\infty}\right)\left(\frac{\tau_{2c}}{\tau_1}\bigg|_{\tau_2\to\infty}\right) < 1. \quad (17)$$

Using expression (13) and its counterpart for $\frac{\tau_{2c}}{\tau_1}|_{\tau_2\to\infty}$, we need to show

$$\left[\frac{1}{\lambda_1\left(D_B^{-1}A\right)}\right]\left[\frac{1}{\lambda_1\left(D_A^{-1}B\right)}\right] < 1. \quad (18)$$

As proved in Sec. 4 of the Appendix, we find that condition (17) is always true except for the special case where node-degree vectors of G_A and G_B are parallel, i.e., $\boldsymbol{d}_A = c\boldsymbol{d}_B$. ■

When dominant eigenvectors of G_A and G_B are not identical, condition (15) indicates that nonaggressive viruses can coexist. Additionally, when propagation of competitive viruses is aggressive, condition (17) indicates viruses can coexist if node-degree vectors of G_A and G_B are not parallel. However, the rare scenario where G_A and G_B are not identical and $\boldsymbol{d}_A = c\boldsymbol{d}_B$ and $\boldsymbol{v}_A = \boldsymbol{v}_B$ hold simultaneously demands further exploration.

The above theorem and Eqs. (11) and (13) prove the importance of the interrelation of network layers. As we discuss in the simulation section, one approach to capture only the effect of interrelation is generating multilayer networks from two graphs G_A and G_B through simple relabeling vertices

of G_B. We thus have a set of multilayer networks whose layers have identical graph properties, but correspondence of nodes in one layer to the nodes of the other varies.

In the context of competitive spreading—whether memes, opinions, or products—the population under study serves as the "resource" for the competitive entities, correlating with the concept of "competing species" in ecology. Long-term study of competing species in ecology centers on the "competitive exclusion principle" [26]: Two species competing for the same resources cannot coexist indefinitely under identical ecological factors. The species with the slightest advantage or edge over another will dominate eventually. Our SI_1SI_2S model also predicts that when the network layers are identical, coexistence is not possible. Significantly, different propagation routes break this "ecological symmetry," allowing coexistence. Not only have we rigorously proved a coexistence region, but we quantitated this ecological asymmetry via interrelation of central nodes across the network layers. None or little overlapping of central nodes of each layer is the key determinant of coexistence. Satisfyingly, this conclusion supports "niche differentiation" in ecology and yet is built upon network science rigor.

C. Standardized threshold diagram and a global approximate formula

Exploring efficient characterization of threshold curves using extreme scenarios, we propose a standardized threshold diagram where threshold curves are plotted in a $[0,1]\times[0,1]$ plane for $(x,y)=[\frac{1}{\lambda_1(B)\tau_2},\frac{1}{\lambda_1(A)\tau_1}]$, and axes are scaled by each layer spectral radius and inverted. Curves in the standardized threshold diagram start from origin and terminate at point (1,1). From (11) and (13), we see the slopes of the survival curve of virus 1 at (0,0) and (1,1) are

$$m_0=\frac{\lambda_1(B)}{\lambda_1(A)}\lambda_1\big(D_B^{-1}A\big), \tag{19}$$

$$m_1=\frac{\sum v_{A,i}^2 v_{B,i}}{\sum v_{B,i}^3}, \tag{20}$$

respectively. Importantly, these slopes help create a parametric approximation of the survival threshold curve $\tau_{1c}=\Phi_1(\tau_2)$ for the full range of τ_2. To do so, we use a quadratic Bézier curve [27] as

$$\begin{bmatrix}x\\y\end{bmatrix}=2\sigma(1-\sigma)\begin{bmatrix}a\\b\end{bmatrix}+\sigma^2\begin{bmatrix}1\\1\end{bmatrix}, \tag{21}$$

connecting $(x,y)=(0,0)$ to $(x,y)=(1,1)$ for $\sigma\in[0,1]$ and satisfying the slope constraints (19) and (20), provided a and b are chosen as

$$a=\frac{1-m_1}{m_0-m_1},\quad b=\frac{m_0(1-m_1)}{m_0-m_1}. \tag{22}$$

Therefore, the Bézier curve (21) approximates the standardized threshold curve diagram for the whole range of $\tau_1>1/\lambda_1(A)$ and $\tau_2>1/\lambda_1(B)$ using only spectral information of a set of matrices.

D. Multilayer network index for competitive spreading

Proving that coexistence is one of the key contributions of this paper. According to (16), we go further to define a topological index $\Gamma_s(\mathcal{G})$ quantifying the possibility of coexistence in a multilayer network $\mathcal{G}=(V,\{E_A,E_B\})$ for the case of nonaggressive spreading as

$$\Gamma_s(\mathcal{G})=1-\frac{\big(\sum v_{B,i}v_{A,i}^2\big)\big(\sum v_{A,i}v_{B,i}^2\big)}{\big(\sum v_{B,i}^3\big)\big(\sum v_{A,i}^3\big)}. \tag{23}$$

Values of $\Gamma_s(\mathcal{G})$ vary from 0 (corresponding to the case where $\boldsymbol{v}_A=\boldsymbol{v}_B$) to 1. In particular, values of $\Gamma_s(\mathcal{G})$ close to zero imply that coexistence is rare, and any surviving virus is indeed the absolute winner. Meanwhile, $\Gamma_s(\mathcal{G})$ closer to 1 indicates that coexistence is very possible on $\mathcal{G}$. Therefore, $\Gamma_s(\mathcal{G})$ can be used to discuss the coexistence of nonaggressive competitive viruses.

Similar to nonaggressive competitive spreading, we can define a topological index $\Gamma_l(\mathcal{G})$ to quantify coexistence possibility in a multilayer network $\mathcal{G}=(V,\{E_A,E_B\})$ as

$$\Gamma_l(\mathcal{G})=1-\left[\frac{1}{\lambda_1\big(D_B^{-1}A\big)}\right]\left[\frac{1}{\lambda_1\big(D_A^{-1}B\big)}\right], \tag{24}$$

according to (18).

Values of $\Gamma_l(\mathcal{G})$ vary from 0 (when $\boldsymbol{d}_A=c\boldsymbol{d}_B$) to 1. Clearly, values of $\Gamma_l(\mathcal{G})$ close to zero imply that coexistence is rare and any surviving virus is indeed the absolute winner, while $\Gamma_l(\mathcal{G})$ closer to 1 indicates coexistence is very possible on $\mathcal{G}$. Therefore, $\Gamma_l(\mathcal{G})$ can be used to discuss the coexistence of aggressive competitive viruses.

E. Numerical simulations

Multilayer network generation. The objective of numerical simulations in this section is not only to test our analytical formulas, but also to investigate our prediction of the cross-layer interrelation effect on competitive epidemics. This task demands a set of two-layer networks for which isolated layers have identical graph properties, but how these layers are interrelated is different, hence capturing the *pure effect of interrelation*. Specifically, in the following numerical simulations, the contact network G_A through which virus 1 propagates is a random geometric graph with $N=1000$ nodes, where pairs at distance less than $r_c=\sqrt{\frac{3\log(N)}{\pi N}}$ connect to ensure connectivity. For the contact graph of virus 2 (G_B), we first generated a scale-free network according to the Barabási-Albert model. We then used a randomized greedy algorithm to associate the nodes of this graph with the nodes of G_A, approaching a certain degree correlation coefficient ρ with G_A; i.e., each iteration step permutates nodes when the degree correlation coefficient,

$$\rho(\mathcal{G})=\frac{\sum(d_{A,i}-\bar{d}_A)(d_{B,i}-\bar{d}_B)}{\sqrt{\sum(d_{A,i}-\bar{d}_A)^2}\sqrt{\sum(d_{B,i}-\bar{d}_B)^2}},$$

is closer to the desired value. Specifically, we obtained three different permutations where the generated graphs are negatively ($\rho=-0.47$), neutrally ($\rho=0$), and positively ($\rho=0.48$) correlated with G_A. These three graphs have *identical graph properties, yet they are distinct respective to*

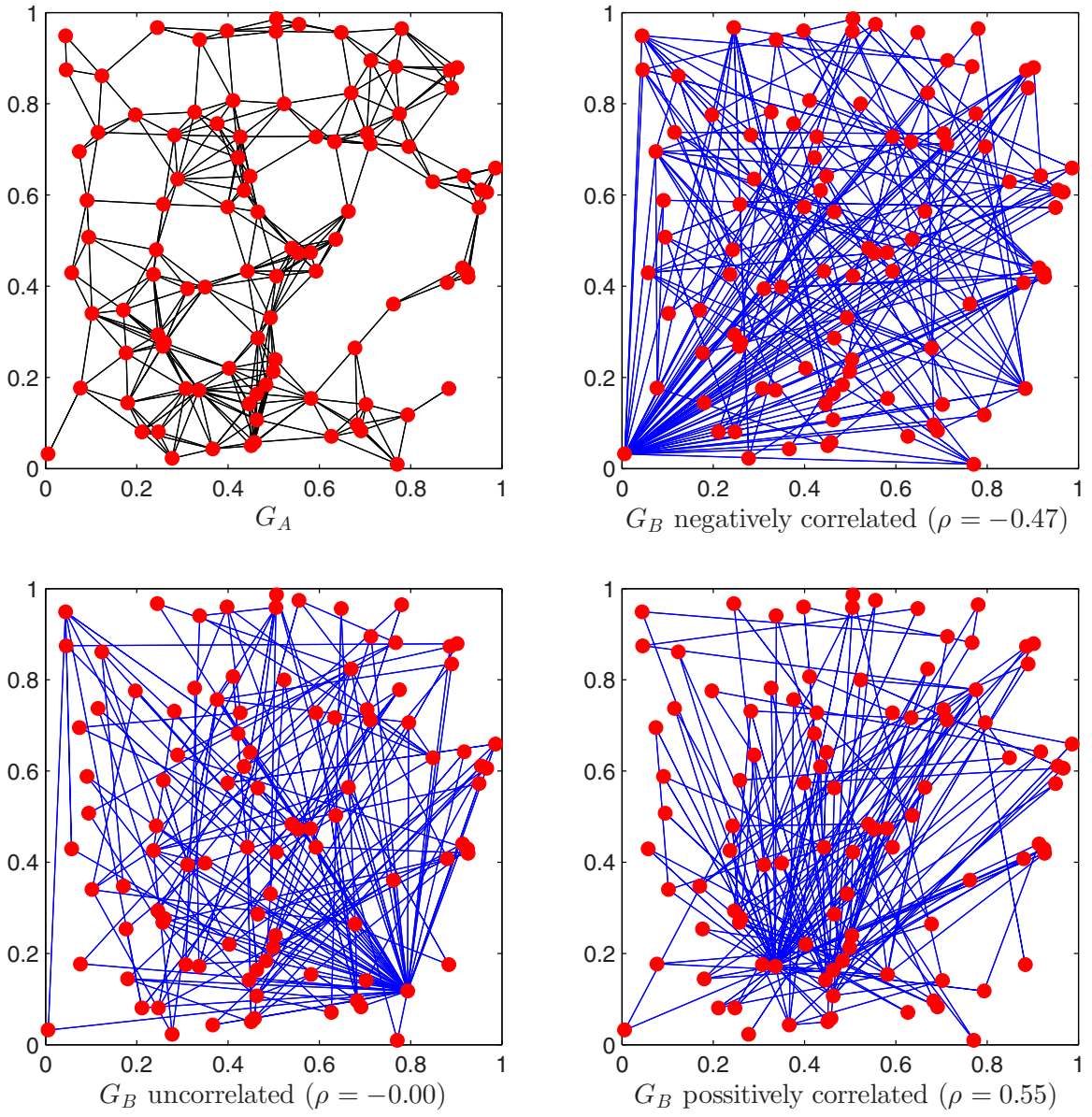

FIG. 9. (Color online) Two-layer network generation for numerical simulations. The contact network G_A through which virus 1 propagates is a random geometric graph where pairs of nodes with a distance less than r_c are connected to each other. For visualization convenience, the number of nodes is $N = 100$, which is different from the actual $N = 1000$ used for numerical simulation results. For the contact graph of virus 2 (G_B), we first generated a scale-free network according to the B-A model, then associated the nodes of this graph with the nodes of G_A to achieve a certain degree correlation coefficient with G_A. Specifically, we obtained three different permutations such that the resultant graphs are negatively, neutrally, or positively correlated with G_A. These three graphs are equivalent if isolated and yet distinct in their interrelation with G_A. The high degree nodes in the positively correlated G_B (bottom right) also have high degree in G_A (top left), while the high degree nodes in the negatively correlated G_B (top right) have low degree size in G_A. The uncorrelated G_B (bottom left) shows no clear association.

G_A. Figure 9 depicts a graph G_A and three graphs of G_B with $N = 100$ nodes for better conceptualization.

Steady-state infection fraction. When two viruses compete to spread, steady-state infection fraction $\bar{p}_1^{ss} = \frac{1}{N}\sum p_{1,i}$ of virus 1 in the SI_1SI_2S model exhibits a threshold behavior at $\tau_1 = \tau_{1c}$, for a given τ_2. Interestingly, aside from the survival threshold τ_{1c}, the absolute-dominance threshold $\tau_1^\dagger$ appears in the figure when plotted against a single-virus case: $\bar{p}_1^{ss}$ takes the same values as the single-virus case for effective infection rates larger than the absolute-dominance threshold $\tau_1^\dagger$, as Fig. 5 shows.

Next, Fig. 10 illustrates the dependency of the steady-state infection fraction curve on network layer interrelation. When the contact network of virus 2 (G_B) is positively correlated with that of virus 1 (G_A), it is more difficult for virus 1 to survive, making the survival threshold τ_{1c} relatively larger for positively correlated G_B. Conversely, negatively correlated contact network layers impede virus 1 from completely

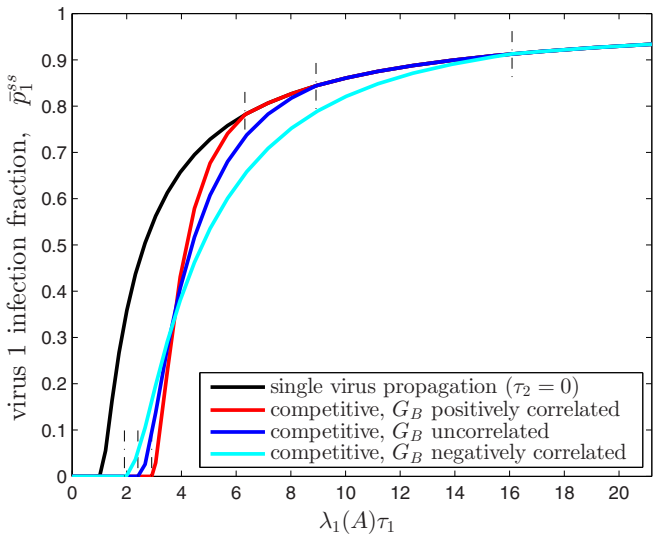

FIG. 10. (Color online) Comparison of steady-state infection fraction curves of virus 1 *in the* SI_1SI_2S *competitive spreading model.* Survival threshold τ_{1c} is larger for positively correlated G_B, indicating that it is more difficult to survive positively correlated G_B, while $\tau_1^\dagger$ is larger for negatively correlated G_B, indicating that it is more difficult to completely suppress the other virus in negatively correlated G_B.

suppressing virus 2, making the absolute-dominance threshold $\tau_1^\dagger$ larger for negatively correlated G_B.

Survival diagram. Allowing for variation of τ_2, the steady-state infection curve extends to the steady-state infection surface. Figure 11 plots the steady-state infection fraction for virus 1 and virus 2 as a function of τ_1 and τ_2. White curves represent theoretical threshold curves derived from the solution to (8), accurately separating the survival regions depicted in Fig. 7.

Finally, Fig. 12 plots the standardized threshold diagrams where G_B is negatively correlated with G_A (left) and G_B is positively correlated with G_A (right). Predictions from the analytical approximation formula (21) estimated the threshold curves fairly accurately.

IV. DISCUSSION AND CONCLUSION

Competitive multivirus propagation shows very rich behaviors, beyond those of single-virus propagation. This type of modeling is suitable for copropagation of opposing opinions about a subject, where people are for, against, or neutral; spreading of a disease through physical contact and viral propagation of antidote providing immunity to the disease; or marketing penetration of competitive products like Android vs Apple smart phones. Aside from its potential applications, the problem of competitive spreading over multilayer networks is technically challenging. In particular, compared to single-layer networks, the science of multilayer networks is still in its infancy, thus warranting research.

A. Physics of competitive spreading on multilayer networks

The definitions of survival and absolute-dominance thresholds enable us to articulate all possible outcomes for the fate of competing viruses. Specifically, the survival threshold of a virus determines the phase transition for that virus from extinction to existence in the competitive environment, while the absolute-dominance threshold denotes the critical point where the virus becomes the sole survivor or absolute winner. Results of this analysis highlighted major differences between a single-layer contact network, where both viruses spread through the same routes, and a multilayer contact network, where each virus has its own transmission route. Significantly, we showed in the case of a single network contact that the phase transition is abrupt, while in the case of the multilayer contact, the phase transitions occur continuously. The abrupt transition occurs because coexistence is not possible for single-layer contact network and a virus either completely dies out or its infection fraction jumps to the positive value of no competition (refer back to Fig. 3). Our results show that the coexistence of

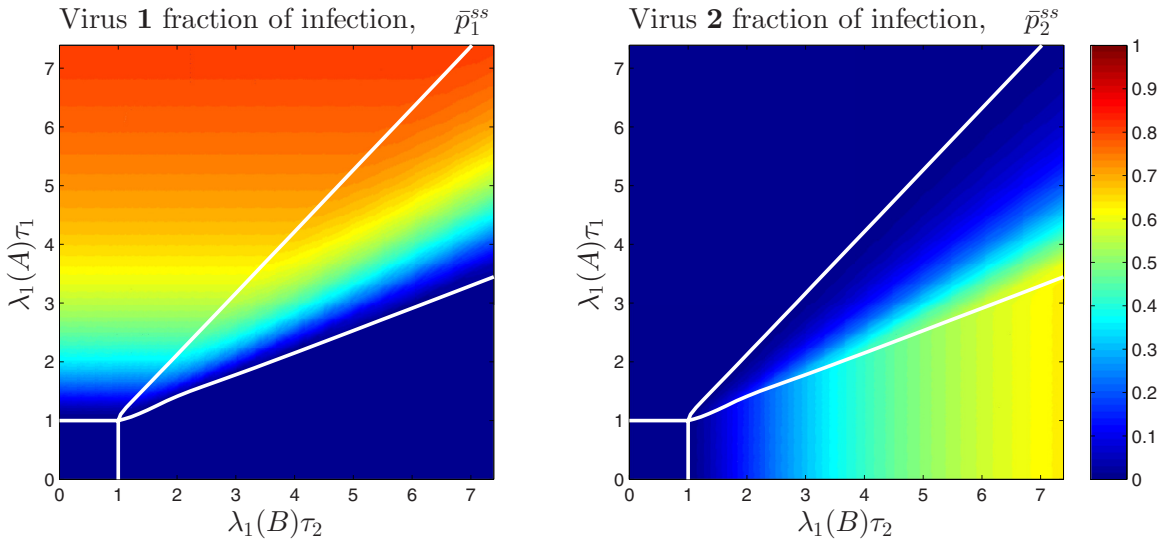

FIG. 11. (Color online) Steady-state fraction of infection for virus 1 (left) and virus 2 (right) as a function of τ_1 *and* τ_2. The white lines are theoretical threshold curves accurately separating the survival regions.

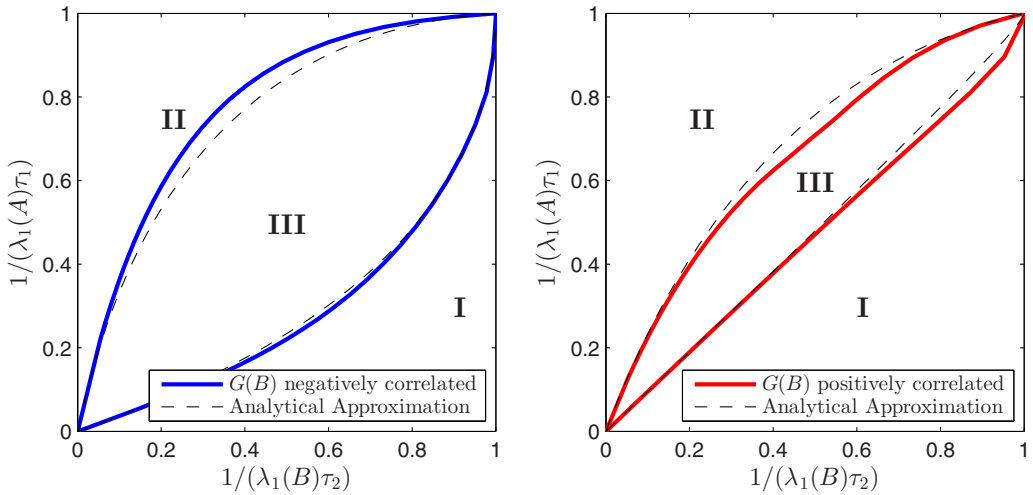

FIG. 12. (Color online) Standardized threshold diagram for the case where G_B is negatively correlated with G_A (left) and the case where G_B is positively correlated with G_A (right). Dashed lines are the predictions from analytical approximation formulas explicitly expressed in (21). The standardized threshold diagram shows three survival regions: virus 1 absolute-dominance region I, where only virus 1 survives and virus 2 dies out; virus 2 absolute-dominance region II, where only virus 2 survives and virus 1 dies out; and finally, coexistence region III, where both viruses survive and persist in the population.

exclusive, competitive viruses is an emergent phenomenon due to the multilayer structure of the underlying contact network. When network layers are identical, the SI_1SI_2S model does not have a coexistence equilibrium point. This result supports the importance of studying the phenomenology of dynamic processes on networks with more complex topologies than static, single-layer graphs. Multilayer and interconnected network modeling has generated interesting results for the case of single-virus spreading (see [28–30], to name a few). As an another example of coexistence, Antunović *et al.* [31] demonstrated the coexistence of competing products when product adoption and network formation would occur concurrently, demonstrating an emergent phenomenon for the preferential attachment-adoption network model.

How interrelation of graph layers of a multilayer network influence dynamical characteristics of processes is very intricate and still open to research and discussion. In the case of the competitive spreading process, the threshold equations (6) and (9) shows an implicit and complex dependency between network layers. However, the eigenvalue perturbation techniques employed in (12) and (14) help unravel the implicit interdependencies of the graph layers. These formulas reveal that no or little overlapping of "central nodes" is a key determinant of the coexistence phase. Interestingly, which nodes are central depends on the dynamical characteristics of the viruses: When the effective infection rates are very high, the central nodes are mainly those with the highest node degrees, and when effective infection rates are close to no-spreading thresholds, the central nodes are those with the highest eigenvector centrality. Clearly, the implication of how node centrality changes depending on the effective infection rates is a promising future research direction.

Moreover, research of aggressive competitive spreading is very important from a practical point of view, as it describes the situation where both viruses are highly contagious in the absence of competition. Interestingly, the survival threshold for aggressive competitive spreading [Eq. (14)] has a very simple and elegant expression. In particular, $\lambda_1(D_B^{-1}A)$ is a new measure for multilayer network structures. The normalized adjacency matrix $D_A^{-1}A$, where each row is divided by the degree of its corresponding node, is well known, particularly in random walks over graphs. Matrix $D_B^{-1}A$ is likewise a normalized adjacency matrix, with the difference that each row of A is divided by the degree of its corresponding node in layer B. However, unlike $D_A^{-1}A$, the matrix $D_B^{-1}A$ is not necessarily a row-stochastic matrix and therefore does not possess well-known properties of stochastic matrices. So far, we have shown that $\lambda_1(D_B^{-1}A)\lambda_1(D_A^{-1}B) > 1$. Studying the properties $D_B^{-1}A$ will further our understanding of competitive viruses, in particular in the more appealing region of aggressive viruses.

B. Scalability to multivirus competitive spreading

A critical challenge regarding modeling and analysis of multivirus spreading is its scalability to a higher number of viruses. Fortunately, our competitive spreading model [Eqs. (1) and (2)] for two viruses can be extended to model multiple virus competitive spreading. In this case, the node state space size is $M+1$; i.e., each node is either susceptible or infected by one of the M viruses [32]. Considering that each virus has its own transmission route, the contact network will be an M-layer network. Thus, M-virus competitive spreading dynamics can be expressed as

$$\dot{p}_{m,i} = \beta_m \left(1 - \sum_{n=1}^{M} p_{n,i}\right) \sum_{j=1}^{N} a_{m,ij}\, p_{m,j} - \delta_m p_{m,i}, \quad m \in \{1,\ldots,M\}, \tag{25}$$

where $p_{m,i}$ is the node i probability of infection by virus m, with infection rate β_m and recovery rate δ_m. Additionally, $a_{m,ij}$ is the adjacency matrix elements of layer m.

Analysis of a competitive spreading scenario with multiple viruses and multiple network layers is technically challenging; however, the scalability issue does correlate directly with the

multilayer network structure. If the contact network has a single layer, then coexistence is not possible, and the winner virus will be the one with the largest effective infection rate. However, as coexistence is possible for the multilayer network scenario, for a system of M competitive viruses, the phase-space size is 2^M; each virus can either survive or die out, and coexistence is possible in a multilayer network. Even so, this exponential explosion of phase space raises technical difficulties for problem analysis. While this paper develops analytical results for competitive spreading of two SIS viruses on a two-layer network, it does not solve the scalability issue upon extensions to multivirus-multilayer competitive spreading. Future research to address the scalability issue, along with relaxing assumptions of complete cross immunity and SIS-like dynamics of this paper, should greatly contribute to a better understanding of spreading processes and the machinery of dynamical processes over multilayer networks.

C. Concluding remarks

In this paper, we study the SI_1SI_2S model, the simplest extension of SIS model to competitive spreading over a two-layer network, focusing on long-term behaviors in relation to multilayer network topology. In brief, the major contributions of this paper are (a) identifying and quantifying extinction, coexistence, and absolute dominance via defining survival thresholds and absolute-dominance thresholds, (b) proving a region of coexistence and quantitating it through overlapping of layers central nodes, (c) developing an explicit approximate formula to globally find threshold values, and (d) proposing a multilayer network generation scheme to capture influence of layers interrelation.

ACKNOWLEDGMENTS

We would like to thank Antonio Scala for insightful discussions and suggestions to improve the manuscript. This work was partially supported by National Science Foundation under Award No. DMS-1201427. Any opinions, findings, or conclusions or recommendations expressed in this paper are those of the authors and do not necessarily reflect the views of the National Science Foundation. This work was also partially supported by the Kansas Bioscience Authority funds to the Institute of Computational Comparative Medicine (ICCM) at Kansas State University.

APPENDIX: SELECTED PROOFS

1. Stability analysis of single-layer network

When $\tau_1 > 1/\lambda_1(A)$ and $\tau_2 > 1/\lambda_1(B)$, the disease free equilibrium $(p^*_{1,i} = 0, p^*_{2,i} = 0)\ \forall\ i \in \{1,\ldots,N\}$ is unstable. The stability of virus 2 absolute-dominance threshold $(p^*_{1,i} = 0, p^*_{2,i} = y_i > 0)\ \forall\ i \in \{1,\ldots,N\}$ can be explored by linearizing (1) at this equilibrium. The linearized system is

$$\dot{\hat{p}}_{1,i} = \beta_1(1-y_i)\sum a_{ij}\hat{p}_{1,j} - \delta_1\hat{p}_{1,i}, \tag{A1}$$

which is stable if all the eigenvalues of $\tau_1\mathrm{diag}\{1-y_i\}A - I$ are negative. Rewriting (6) for $B = A$ as

$$y_i = \tau_2(1-y_i)\sum a_{ij}y_j \tag{A2}$$

suggests that zero is the largest eigenvalue of $\tau_2\mathrm{diag}\{1-y_i\}A - I$. Therefore, for $\tau_1 < \tau_2$, all the eigenvalues of $\tau_1\mathrm{diag}\{1-y_i\}A - I$ are negative; thus, the virus 2 absolute-dominance equilibrium is stable. Similarly, the virus 1 absolute-dominance equilibrium is stable if $\tau_1 > \tau_2$. Therefore, for $\tau_1 \neq \tau_2$, exactly only one of the absolute-dominance equilibriums is stable.

2. Derivation of threshold equation

Differentiating equilibrium equation (3) with respect to τ_1 yields

$$\frac{\frac{dp^*_{1,i}}{d\tau_1}(1-p^*_{2,i}) + p^*_{1,i}\frac{dp^*_{2,i}}{d\tau_1}}{(1-p^*_{1,i}-p^*_{2,i})^2} = \tau_1\sum a_{ij}\frac{dp^*_{1,j}}{d\tau_1} + \sum a_{ij}p^*_{1,j}. \tag{A3}$$

At the survival threshold, $\tau_1 = \tau_{1c}$, $p^*_{1,i} = 0$, and $p^*_{2,i} = y_i$ from (6). Substituting these values in (A3),

$$\frac{1}{(1-y_i)}\frac{dp^*_{1,i}}{d\tau_1}\bigg|_{\tau_1=\tau_{1c}} = \tau_{1c}\sum a_{ij}\frac{dp^*_{1,j}}{d\tau_1}\bigg|_{\tau_1=\tau_{1c}}. \tag{A4}$$

Reexpressing the above equation, we get

$$\frac{dp^*_{1,i}}{d\tau_1}\bigg|_{\tau_1=\tau_{1c}} = \tau_{1c}(1-y_i)\sum a_{ij}\frac{dp^*_{1,j}}{d\tau_1}\bigg|_{\tau_1=\tau_{1c}}, \tag{A5}$$

which is equivalent to (8) according to definition (7). A similar stability analysis technique in Sec. 1 of this appendix proves that the virus 2 absolute-dominance equilibrium is unstable if $\tau_1 > \tau_{1c}$. Therefore, if $\tau_1 > \tau_{1c}$ and $\tau_2 > \tau_{2c}$, disease-free and absolute-dominance equilibriums will all be unstable and the system will go to the coexistence equilibrium.

3. Derivation of eigenvalue perturbation formulas

Here we detail the derivations of (11) and (13). At $\tau_2 = 1/\lambda_1(B)$, (6) finds $y_i = 0$ for all nodes. Equation (6) is indeed the steady-state equation for infection probabilities in the NIMFA model. Van Mieghem [21] found for the SIS model the derivative with respect to effective infection rate, suggesting

$$\frac{dy_i}{d\tau_2}\bigg|_{\tau_2=\frac{1}{\lambda_1(B)}} = c_B v_{B,i}, \tag{A6}$$

$$w_i|_{\tau_2=\frac{1}{\lambda_1(B)}} = c_A v_{A,i}, \tag{A7}$$

where

$$c_A = \frac{\lambda_1(A)}{\sum v^3_{A,i}}, c_B = \frac{\lambda_1(B)}{\sum v^3_{B,i}}, \tag{A8}$$

where v_A and v_B are the normalized dominant eigenvectors of A and B, respectively.

Differentiating (8) with respect to τ_2 yields

$$\begin{aligned}\frac{dw_i}{d\tau_2} &= \frac{d\tau_{1c}}{d\tau_2}(1-y_i)\sum a_{ij}w_j \\ &+ \tau_{1c}\left(-\frac{dy_i}{d\tau_2}\right)\sum a_{ij}w_j \\ &+ \tau_{1c}(1-y_i)\sum a_{ij}\frac{dw_j}{d\tau_2}.\end{aligned} \tag{A9}$$

Inserting $\tau_{1c} = 1/\lambda_1(A)$, $w_i = c_A v_{A,i}$, $y_i = 0$, and $dy_i/d\tau_2 = c_B v_{B,i}$, the above equation changes to

$$\left[I - \frac{1}{\lambda_1(A)}A\right]\frac{d\boldsymbol{w}}{d\tau_2} = \left(\frac{d\tau_{1c}}{d\tau_2}\right)\lambda_1(A)c_A\boldsymbol{v}_A - c_B c_A(\boldsymbol{v}_B \circ \boldsymbol{v}_A) \tag{A10}$$

in the collective form, where the Hadamard product $\circ$ acts entrywise. Multiplying both sides by v_A^T from the left yields

$$\left.\frac{d\tau_{1c}}{d\tau_2}\right|_{\tau_2=\frac{1}{\lambda_1(B)}} = \frac{1}{\lambda_1(A)}c_B\boldsymbol{v}_A^T(\boldsymbol{v}_B \circ \boldsymbol{v}_A) = \frac{\lambda_1(B)}{\lambda_1(A)}\frac{\sum v_{A,i}^2 v_{B,i}}{\sum v_{B,i}^3}, \tag{A11}$$

obtaining (11). Finding $\frac{d\tau_{1c}}{d\tau_2}$ at $\tau_2 = 1/\lambda_1(B)$ obtains the dependence of τ_{1c} on τ_2 close to $1/\lambda_1(B)$.

Replacing for $1 - y_i = \frac{\tau_2^{-1}}{\tau_2^{-1}+\sum b_{ij}y_j}$ from (6) into (8) yields

$$w_i = \left(\frac{\tau_{1c}}{\tau_2}\right)\left(\frac{1}{\tau_2^{-1} + \sum b_{ij}y_j}\right)\sum a_{ij}w_j. \tag{A12}$$

When the effective infection rate τ_2 is enormous $\tau_2^{-1} \to 0$ and $y_i \to 1$, suggesting

$$w_i = \left(\frac{\tau_{1c}}{\tau_2}|_{\tau_2\to\infty}\right)\frac{1}{d_{B,i}}\sum a_{ij}w_j, \tag{A13}$$

where $d_{B,i}$ is the B degree of node i. Therefore, $\frac{\tau_{1c}}{\tau_2}|_{\tau_2\to\infty}$ is the inverse of the spectral radius of $D_B^{-1}A$, proving (13) for large values of τ_2.

4. Coexistence proofs

a. Coexistent region nonaggressive competitive viruses

To investigate the coexistence region for nonaggressive viruses, we show that (15) is true. From (11), we find

$$\left.\frac{d\tau_{1c}}{d\tau_2}\frac{d\tau_{2c}}{d\tau_1}\right|_{(\tau_1,\tau_2)=[\frac{1}{\lambda_1(A)},\frac{1}{\lambda_1(B)}]} = \frac{\left(\sum v_{B,i}v_{A,i}^2\right)\left(\sum v_{A,i}v_{B,i}^2\right)}{\left(\sum v_{B,i}^3\right)\left(\sum v_{A,i}^3\right)}. \tag{A14}$$

Proposition 1 (Hölder's inequality [33]). For $p,q > 0$ satisfying $\frac{1}{p} + \frac{1}{q} = 1$,

$$\sum_{i=1}^n |x_i y_i| \leqslant \left(\sum_{i=1}^n |x_i|^p\right)^{1/p}\left(\sum_{i=1}^n |y_i|^q\right)^{1/q}$$

is always true for $x, y \in \mathbb{R}^n$. The equality happens if and only if $x = y$.

Selecting $p = 3, q = 3/2$, we apply the Hölder's inequality to get

$$\sum v_{B,i}v_{A,i}^2 \leqslant \left(\sum v_{B,i}^3\right)^{1/3}\left[\sum (v_{A,i}^2)^{3/2}\right]^{1/\frac{3}{2}} = \left(\sum v_{B,i}^3\right)^{1/3}\left(\sum v_{A,i}^3\right)^{2/3}, \tag{A15}$$

and similarly for $p = 3/2, q = 3$, we obtain

$$\sum v_{A,i}v_{B,i}^2 \leqslant \left(\sum v_{B,i}^3\right)^{2/3}\left(\sum v_{A,i}^3\right)^{1/3}, \tag{A16}$$

and the equality happens if and only if $\boldsymbol{v}_A = \boldsymbol{v}_B$. Multiplying sides of (A15) and (A16) yields

$$\left(\sum v_{B,i}v_{A,i}^2\right)\left(\sum v_{A,i}v_{B,i}^2\right) \leqslant \left(\sum v_{B,i}^3\right)\left(\sum v_{A,i}^3\right), \tag{A17}$$

proving that (15) is true if $\boldsymbol{v}_A \neq \boldsymbol{v}_B$.

b. Coexistent region for aggressive competitive viruses

To investigate the coexistence region for nonaggressive viruses we shown that (15) is true. Substituting from (13) yields

$$\left(\frac{\tau_{1c}}{\tau_2}|_{\tau_2\to\infty}\right)\left(\frac{\tau_{2c}}{\tau_1}|_{\tau_1\to\infty}\right) = \left[\frac{1}{\lambda_1(D_B^{-1}A)}\right]\left[\frac{1}{\lambda_1(D_A^{-1}B)}\right] = \frac{1}{\lambda_1\left(D_B^{-1}A \otimes D_A^{-1}B\right)} = \frac{1}{\lambda_1\left[\left(D_B^{-1}\otimes D_A^{-1}\right)(A\otimes B)\right]} = \frac{1}{\lambda_1[(D_B\otimes D_A)^{-1}(A\otimes B)]}, \tag{A18}$$

according to properties of the Kronecker product (see [34]).

The degree diagonal matrix of $(A \otimes B)$ is $(D_A \otimes D_B)$. Therefore, $(D_B \otimes D_A)$ is a diagonal permutation of the degree diagonal matrix of $(A \otimes B)$. According to Lemma 1, presented in the following, $\lambda_1[(D_B \otimes D_A)^{-1}(A \otimes B)] \geqslant 1$; thus,

$$\left(\frac{\tau_{1c}}{\tau_2}|_{\tau_2\to\infty}\right)\left(\frac{\tau_{2c}}{\tau_1}|_{\tau_1\to\infty}\right) \leqslant 1, \tag{A19}$$

and equality holds only if $D_B \otimes D_A = D_A \otimes D_B$, which holds only if ratio of B degree and A degree of each node is the same for all nodes.

Lemma 1. If $H = \pi(D_C)^{-1}C$, where $\pi(D_C)$ is a diagonal permutation of degree diagonal matrix of symmetric matrix C, then $\lambda_1(H) \geqslant 1$. Furthermore, equality holds only if $\pi(D_C) = D_c$.

Proof. The largest eigenvalue maximizes the Rayleigh quotient; therefore,

$$\lambda_1(H) = \lambda_1[\pi(D_C)^{-1}C] = \lambda_1[\pi(D_C)^{-1/2}C\pi(D_C)^{-1/2}] = \max_x \frac{x^T\pi(D_C)^{-1/2}C\pi(D_C)^{-1/2}x}{x^Tx} \geqslant \frac{1^TC1}{1^T\pi(D_C)1} = \frac{\sum d_{C,i}}{\sum d_{C,\pi_i}} = 1,$$

where d_{C,π_i} is the degree of node i map. Therefore, $\lambda_1(H) \geqslant 1$. Equality holds only if $x = \pi(D_C)^{1/2}1$ is the dominant eigenvector of $\pi(D_C)^{-1/2}C\pi(D_C)^{-1/2}$, i.e., $\pi(D_C)^{-1/2}C1 = \pi(D_C)^{1/2}1$, which only holds if $d_{C,\pi_i} = d_{C,i}$. ■

5. Steady-state numerical solution

Given $\tau_2 > 1/\lambda_1(B)$, (8) and (6) numerically find $\tau_{1,c}$. We now define $x_i \triangleq \frac{y_i}{1-y_i}$, given the recursive iteration law,

$$x_i(k+1) = \tau_2 \sum b_{ij} \frac{x_j(k)}{1+x_j(k)}, \tag{A20}$$

to prove they converge exponentially, numerically solving (6) as $\frac{x_i(k)}{1+x_i(k)} \to y_i$. The main advantage of finding equilibrium values using recursive law (A20) instead of solving ordinary differential equations of the model is that recursive law (A20) does not require any incremental time increase, making computations significantly faster.

Furthermore, the steady-state infection probabilities in (3) and (4) can be found via the recursive iteration law,

$$x_{1,i}(k+1) = \tau_1 \sum a_{ij} \frac{x_{1,j}(k)}{1+x_{1,j}(k)+x_{2,j}(k)}, \tag{A21}$$

$$x_{2,i}(k+1) = \tau_2 \sum b_{ij} \frac{x_{2,j}(k)}{1+x_{1,j}(k)+x_{2,j}(k)}, \tag{A22}$$

for which $\frac{x_{1,j}(k)}{1+x_{1,j}(k)+x_{2,j}(k)} \to p^*_{1,i}$ and $\frac{x_{2,j}(k)}{1+x_{1,j}(k)+x_{2,j}(k)} \to p^*_{2,i}$ as $k \to \infty$.

[1] B. Karrer and M. E. J. Newman, Phys. Rev. E **84**, 036106 (2011).

[2] S. Funk and V. A. A. Jansen, Phys. Rev. E **81**, 036118 (2010).

[3] Y.-Y. Ahn, H. Jeong, N. Masuda, and J. D. Noh, Phys. Rev. E **74**, 066113 (2006).

[4] X. Wei, N. C. Valler, B. A. Prakash, I. Neamtiu, M. Faloutsos, and C. Faloutsos, IEEE J. Sel. Areas Commun. **31**, 1049 (2013).

[5] S. Aral and D. Walker, Management Sci. **57**, 1623 (2011).

[6] L. Weng, A. Flammini, A. Vespignani, and F. Menczer, Sci. Rep. **2**, 335 (2012).

[7] S. A. Myers and J. Leskovec, in *IEEE 12th International Conference on Data Mining (ICDM), 2012, Brussels* (IEEE Computer Society, New York, 2012), pp. 539–548.

[8] S. Shrestha, A. A. King, and P. Rohani, PLoS Comput. Biol. **7**, e1002135 (2011).

[9] C. Poletto, S. Meloni, V. Colizza, Y. Moreno, and A. Vespignani, PLoS Comput. Biol. **9**, e1003169 (2013).

[10] M. Newman and C. R. Ferrario, PloS One **8**, e71321 (2013).

[11] C. Granell, S. Gómez, and A. Arenas, Phys. Rev. Lett. **111**, 128701 (2013).

[12] M. E. J. Newman, Phys. Rev. Lett. **95**, 108701 (2005)

[13] Q. Wu, M. Small, and H. Liu, J. Nonlinear Sci. **23**, 113 (2012).

[14] Y. Wang, G. Xiao, and J. Liu, New J. Phys. **14**, 013015 (2012).

[15] B. A. Prakash, A. Beutel, R. Rosenfeld, and C. Faloutsos, in *Proceedings of the 21st International Conference on World Wide Web* (ACM, New York, 2012), pp. 1037–1046.

[16] A. Beutel, B. A. Prakash, R. Rosenfeld, and C. Faloutsos, in *Proceedings of the 18th ACM SIGKDD International Conference on Knowledge Discovery and Data Mining* (ACM, New York, 2012), pp. 426–434.

[17] X. Wei, N. Valler, B. A. Prakash, I. Neamtiu, M. Faloutsos, and C. Faloutsos, ACM SIGCOMM Comput. Commun. Rev. **42**, 5 (2012).

[18] Wei *et al.* [4] defined the first eigenvalue of a meme as $\boldsymbol{\beta}\lambda_1 - \boldsymbol{\delta}$, where $\boldsymbol{\beta}$ is infection probability, $\boldsymbol{\delta}$ is curing probability, and λ_1 is spectral radius of the underlying graph layer.

[19] A graph property is any property on a graph that is invariant under relabeling of nodes. Eigenvalues, degree moments, graph diameter, etc., are examples of graph properties.

[20] Wei *et al.* [17] referred to their model as SI_1I_2S. We prefer SI_1SI_2S as it better emphasizes the impossibility of direct transition between I_1 and I_2 in this model.

[21] P. Van Mieghem, J. Omic, and R. Kooij, IEEE/ACM Trans. Networking **17**, 1 (2009).

[22] A. Ganesh, L. Massoulie, and D. Towsley, in *Proceedings of the IEEE 24th Annual Joint Conference of the IEEE Computer and Communications Societies, INFOCOM, 2005* (IEEE, Piscataway, NJ, 2005), Vol. 2, pp. 1455–1466.

[23] E. Cator, R. van de Bovenkamp, and P. Van Mieghem, Phys. Rev. E **87**, 062816 (2013).

[24] F. Sahneh, C. Scoglio, and P. Van Mieghem, IEEE/ACM Trans. Networking **21**, 1609 (2013).

[25] In the context of infectious disease propagation, "highly contagious" is a common terminology to describe a virus with a very large basic reproduction number. Since the cross-immunity assumption in our SI_1SI_2S model fits better to product competition interpretations, we describe competition between highly contagious viruses as "aggressive."

[26] G. Hardin *et al.*, Science **131**, 1292 (1960).

[27] R. H. Bartels, J. C. Beatty, and B. A. Barsky, *An Introduction to Splines for Use in Computer Graphics and Geometric Modeling*, The Morgan Kaufmann Series in Computer Graphics (Morgan Kaufmann Publishers Inc., San Francisco, CA, 1987).

[28] E. Cozzo, R. A. Banos, S. Meloni, and Y. Moreno, Phys. Rev. E **88**, 050801 (2013).

[29] F. D. Sahneh, C. Scoglio, and F. N. Chowdhury, in *American Control Conference (ACC), 2013, Washington, DC* (IEEE, Piscataway, NJ, 2013), pp. 2307–2312.

[30] H. Wang, Q. Li, G. DAgostino, S. Havlin, H. E. Stanley, and P. Van Mieghem, Phys. Rev. E **88**, 022801 (2013).

[31] T. Antunović, E. Mossel, and M. Z. Rácz, arXiv:1307.2893.

[32] In general case of interacting multivirus problem, the problem setup is cumbersome because each node state has 2^M possibilities, as a node might be infected by multiple viruses simultanously. However, in the special case of competitive spreading, the problem setup is no longer problematic as a node can only be infected by just one virus at any instance.

[33] Z. Cvetkovski, *Inequalities: Theorems, Techniques and Selected Problems* (Springer, Berlin, 2012).

[34] A. Graham, *Kronecker Products and Matrix Calculus: With Applications* (Ellis Horwood Ltd., Chichester, UK, 1981).